Supporting

Doped thieno[3,4-b]thiophene -based copolymers for p-type organic thermoelectric materials

Sicheng Wu[a, b], Weilong Xing[a, b], Mengsu Zhu[a, b], Yimeng Sun[a], Ye Zou[a], Wei Xu[*, a, b], Daoben Zhu[*, a, b].

[a] Beijing National Laboratory for Molecular Sciences, Key Laboratory of Organic Solids, Institute of Chemistry, Chinese Academy of Sciences, Beijing, 100190, China.

[b] University of Chinese Academy of Sciences, Beijing, 100049, China.

[*]Corresponding author.

Email addresses: wxu@iccas.ac.cn (W. Xu). zhudb@iccas.ac.cn (D.B. Zhu)

1. Measurements

TGA curves were obtained under the N_2 flow by a TGA Q500 instrument with a heating rate of 10 °C min^{-1}. CV measurements were conducted on a CHI660C electrochemical workstation with 0.1 M Bu_4NPF_6 anhydrous acetonitrile solution as supporting electrolyte at a scan rate of 50 mV s^{-1}, using platinum as a counter electrode, glassy carbon as a working electrode, and Ag/AgCl as a reference electrode. UV-vis spectra were recorded on a JASCO V-570 UV/vis/NIR spectrometer at RT. XRD was measured on D/max2500. XPS and UPS were measured via an AXIS Ultra-DLD ultrahigh vacuum photoemission spectroscopy system (Kratos Co.).

2. Supporting Figures

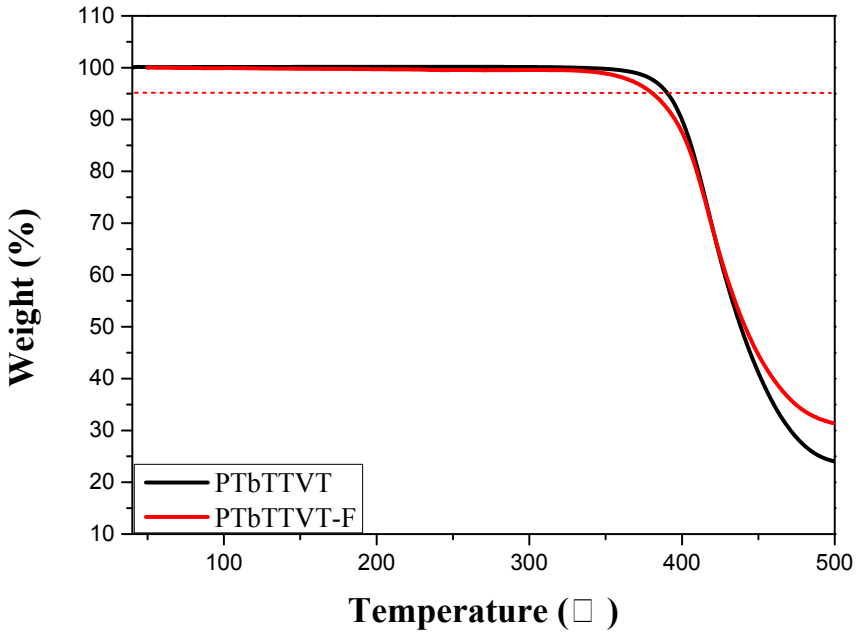

Fig. S1. TGA curves of PTbTTVT and PTbTTVT-F with a heating rate of 10 °C min^{-1}.

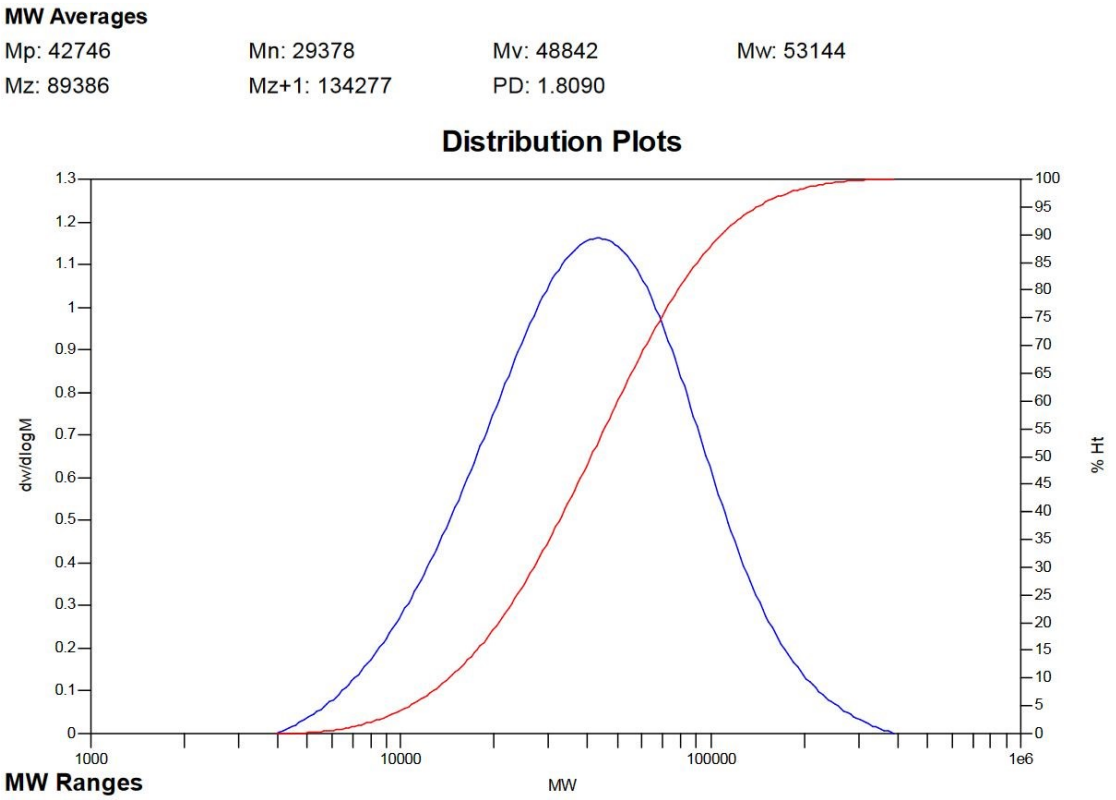

Fig. S2. GPC curves of PTbTTVT.

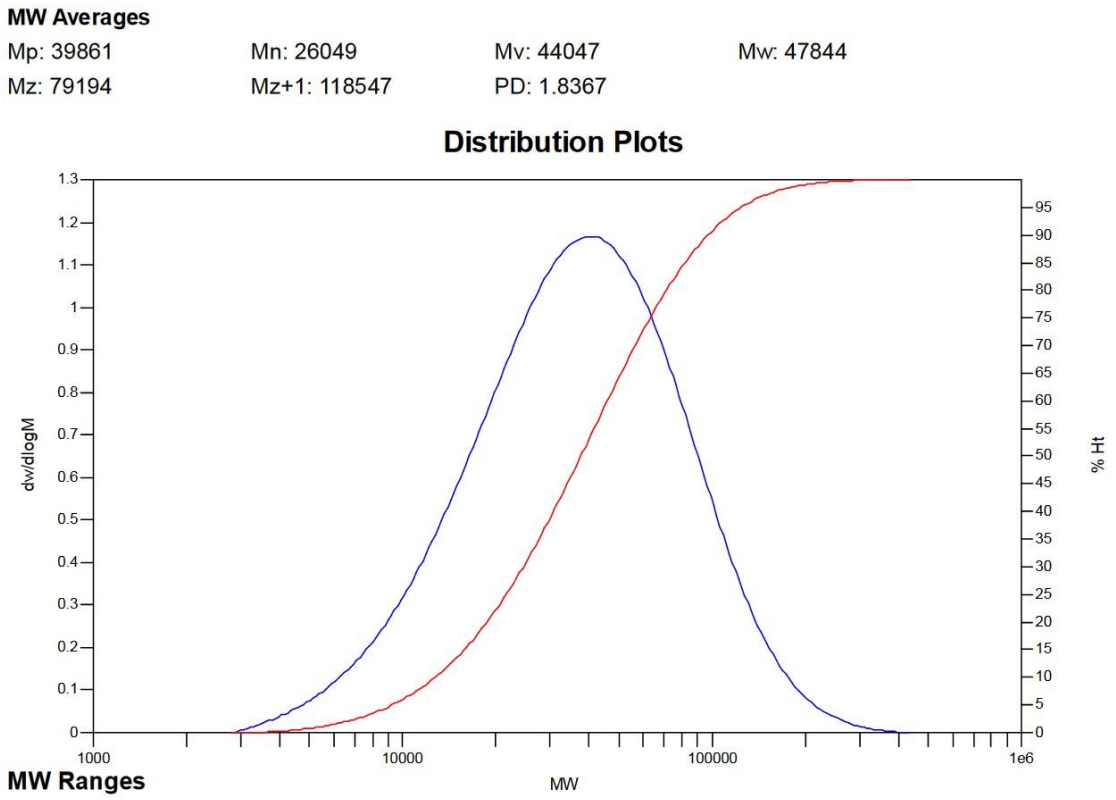

Fig. S3. GPC curves of PTbTTVT-F.

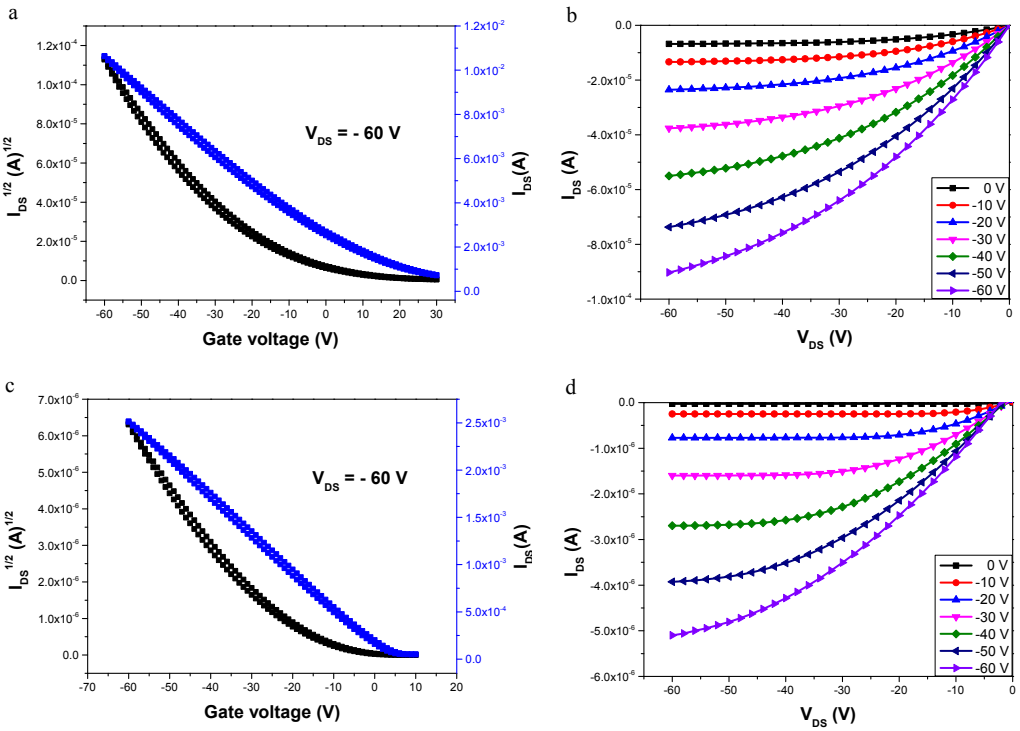

Fig. S4. Typical transfer (left) and output (right) curves based on TbT-based polymer devices. (a)(b): PTbTTVT, (c)(d): PTbTTVT-F.

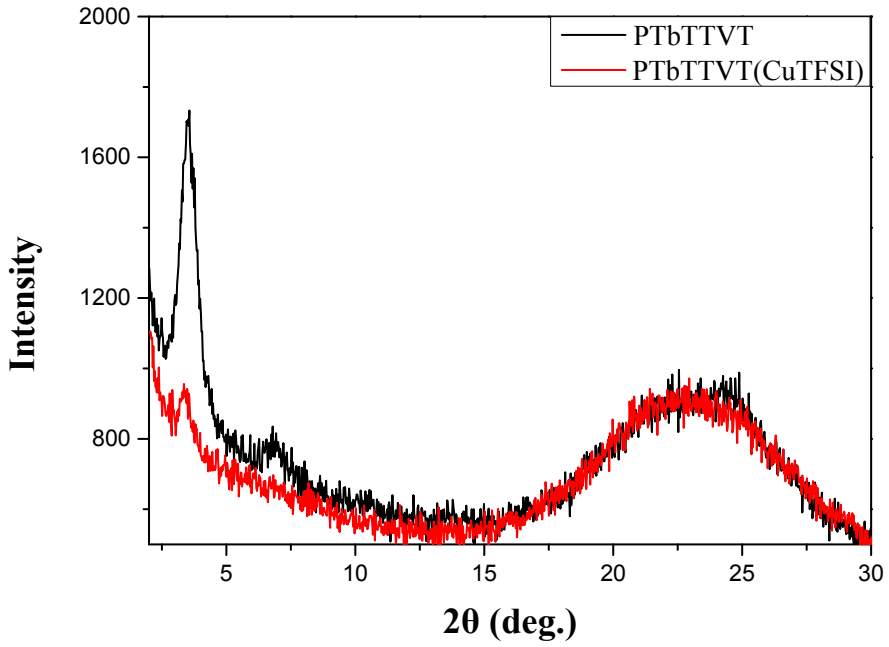

Fig. S5. XRD patterns of PTbTTVT before and after CuTFSI doping.

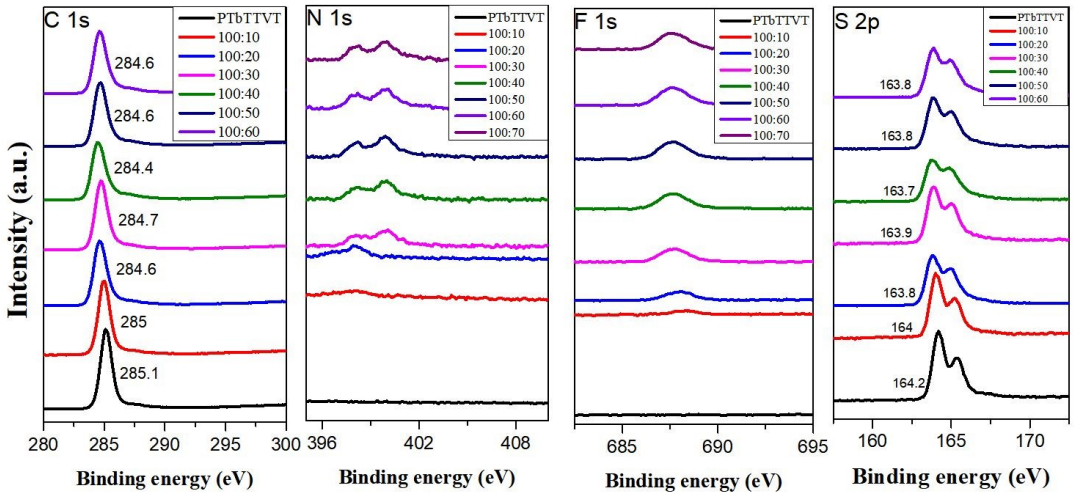

Fig. S6. XPS spectra of PTbTTVT with undoped and different F4TCNQ doped concentrations, (a) C (1s), (b) N (1s), (c) F (1s), (d) S (2p)

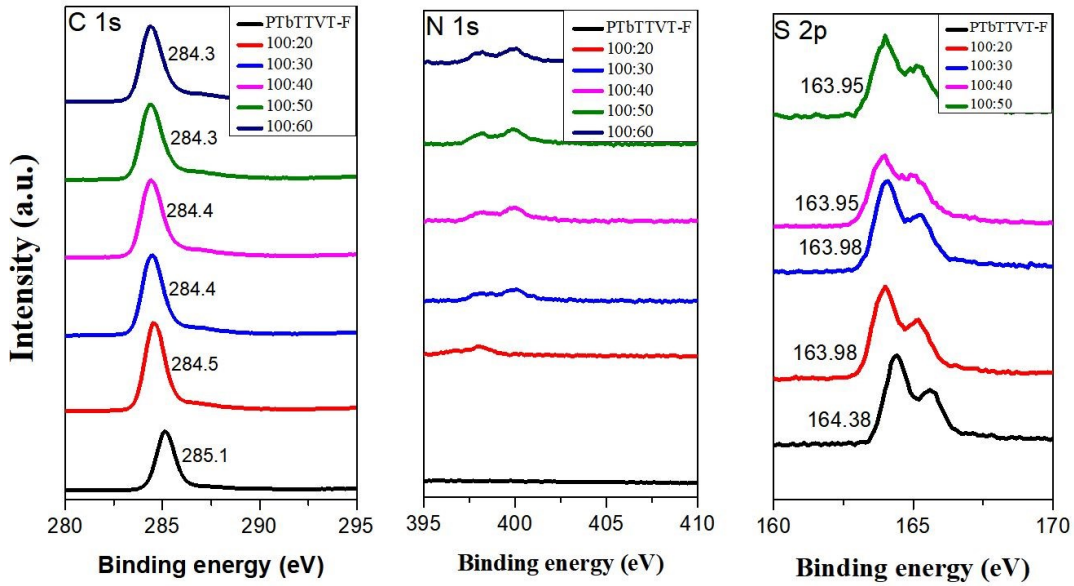

Fig. S7. XPS spectra of PTbTTVT-F with undoped and different F4TCNQ doped concentrations, (a) C (1s), (b) N (1s), (c) S (2p).

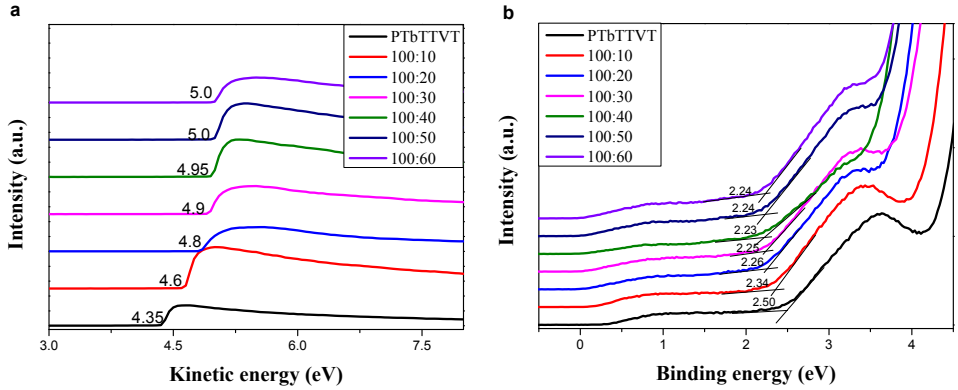

Fig. S8. UPS spectra of PTbTTVT with undoped and different F4TCNQ doped concentrations,

(a) spectra of low kinetic energy region, (b) spectra of low binding energy region (HOMO).

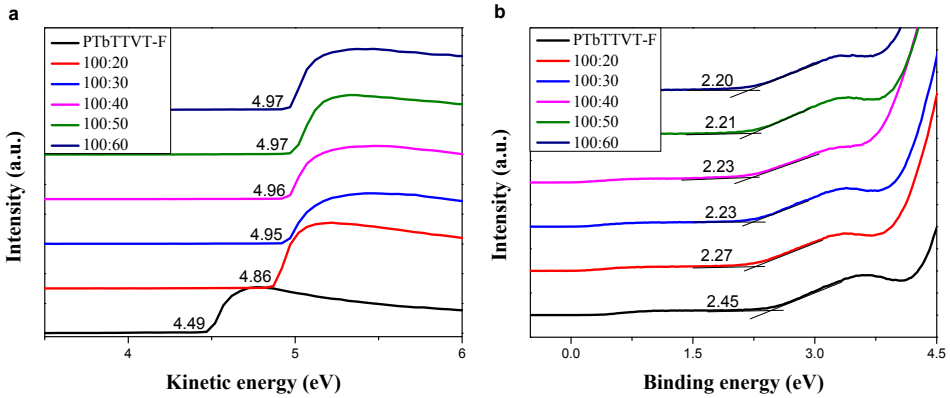

Fig. S9. UPS spectra of PTbTTVT-F with undoped and different F4TCNQ doped concentrations, (a) spectra of low kinetic energy region, (b) spectra of low binding energy region (HOMO).

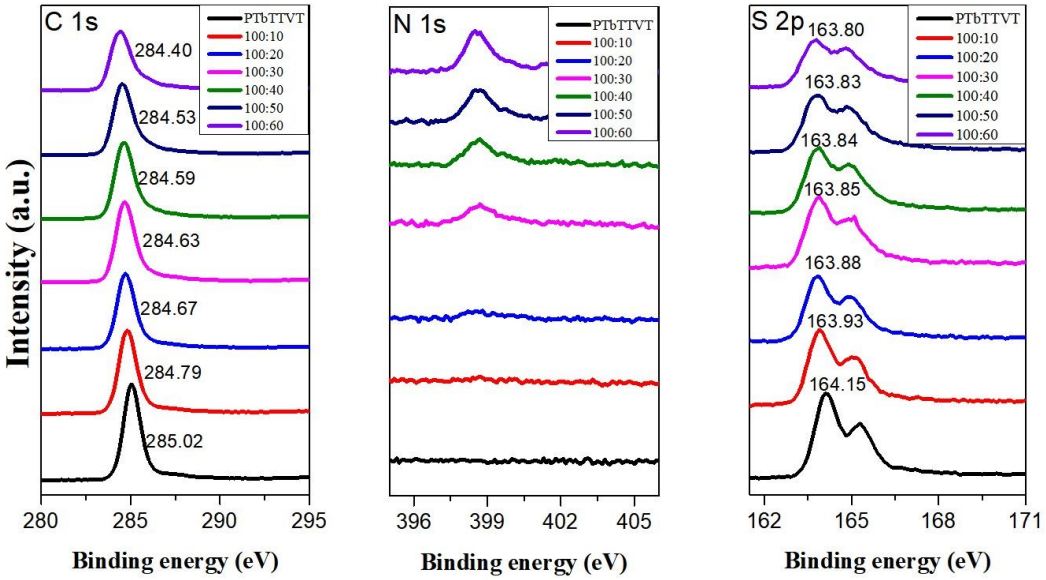

Fig. S10. XPS spectra of PTbTTVT with undoped and different CN6CP doped concentrations, (a) C (1s), (b) N (1s), (c) S (2p).

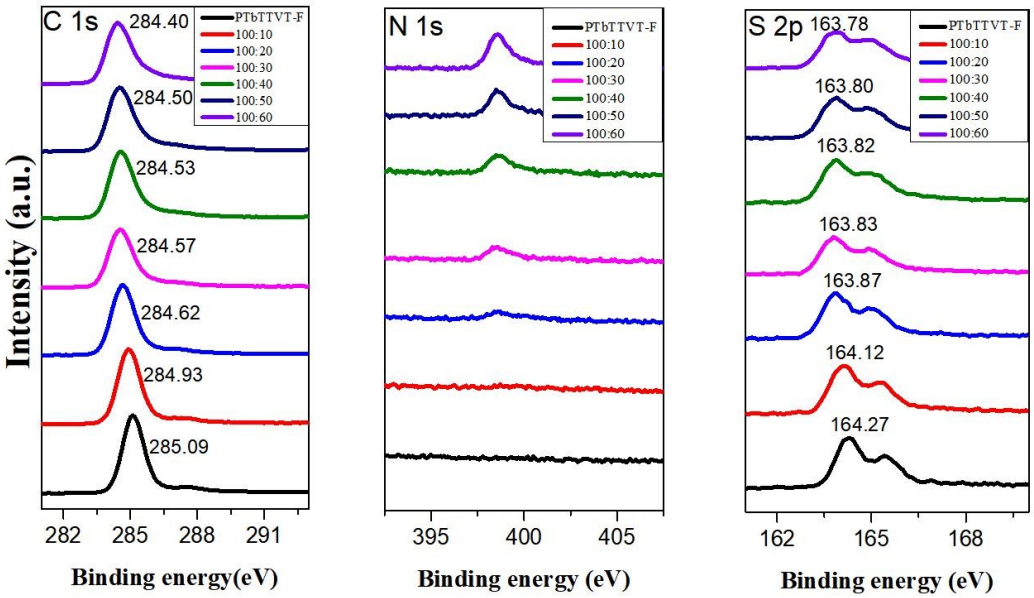

Fig. S11. XPS spectra of PTbTTVT-F with undoped and different CN6CP doped concentrations, (a) C (1s), (b) N (1s), (c) S (2p).

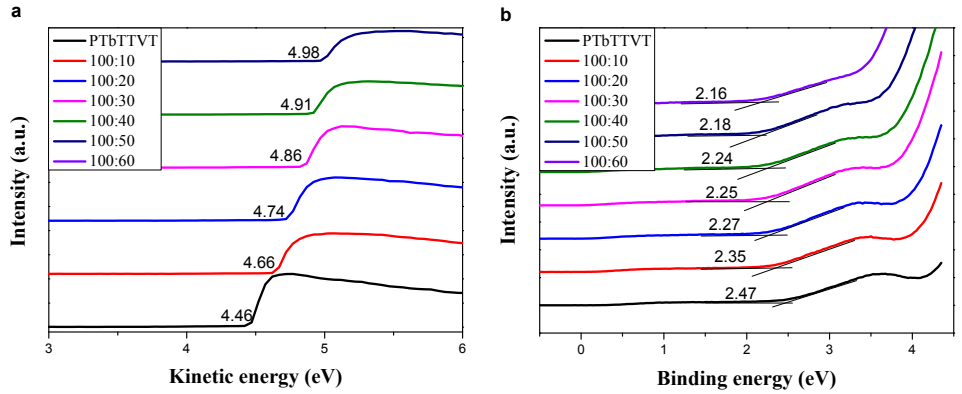

Fig. S12. UPS spectra of PTbTTVT with undoped and different CN6CP doped concentrations, (a) spectra of low kinetic energy region, (b) spectra of low binding energy region (HOMO).

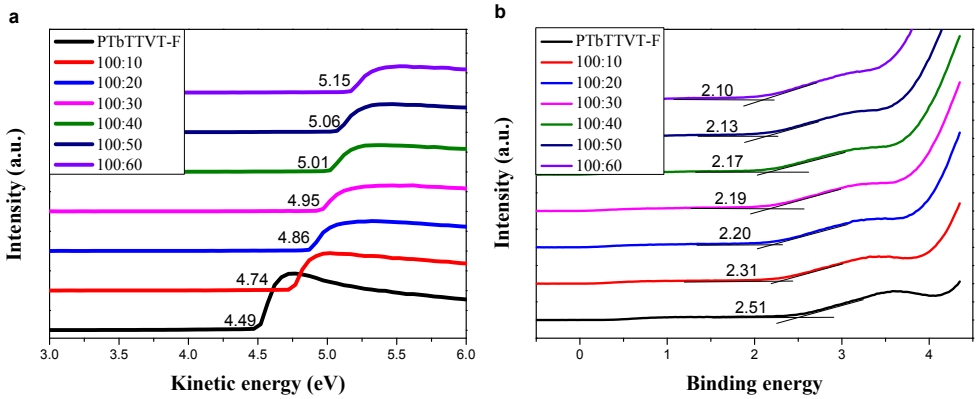

Fig. S13. UPS spectra of PTbTTVT-F with undoped and different CN6CP doped concentrations, (a) spectra of low kinetic energy region, (b) spectra of low binding energy region (HOMO).

Table S1. Dihedral angles between aromatic subunits of oligomers O1 and O2.

Label of two aromatic subunits	AB	BC	CD	BE
O1	166.0	178.2	166.4	166.9
O2	163.3	174.3	165.9	166.1